Reversible Zn^{2+}-induced 3D self-assembly aerogel of carboxyl modified copper indium diselenide quantum dots：mechanism and application for inkjet printing anti-counterfeiting

Jilei Chen [a], Wenrong Fu [a], Jiaqiang Xiong [b], Wei Zhang [b], Feng-Lei Jiang [a], Liuchun Zheng [c,], Yi Liu [a,c,d,*], Peng Jiang [a,*]*

[a] Key Laboratory of Combinatorial Biosynthesis and Drug Discovery (MOE), College of Chemistry and Molecular Sciences & School of Pharmaceutical Sciences, Wuhan University, Wuhan 430072, P. R. China.

[b] Department of Obstetrics and Gynecology, Zhongnan Hospital, Wuhan University, Wuhan 430072, P. R. China

[c] State Key Laboratory of Separation Membranes and Membrane Process, School of Textile & School of Chemistry, Tiangong University, Tianjin 300387, P. R. China

[d] Institute of Advanced Materials and Nanotechnology & Hubei Province Key Laboratory for Coal Conversion and New Carbon Materials, College of Chemistry and Chemical Engineering, Wuhan University of Science and Technology, Wuhan 430081, P. R. China

Contents

Table S1 Lifetimes fitting data of CISe QDs, Zn-CISe gel and Zn-CISe aerogel.

	τ_1 (ns)	A_1	τ_2 (ns)	A_2	τ_3 (ns)	A_3	τ_{ave} (ns)	R^2
CISe QDs	9.0	34%	76.7	37%	268.8	29%	210.8	0.9992
Zn-CISe gel	18.2	13%	123.3	55%	310.0	33%	232.5	0.9994
Zn-CISe aerogel	203.4	77%	606.8	23%	-	-	391.4	0.9993

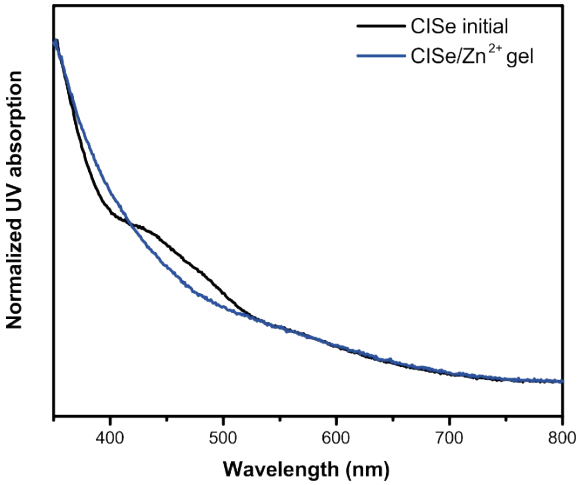

Figure S1 UV-vis absorption of CISe QDs and Zn-CISe QDs gel.

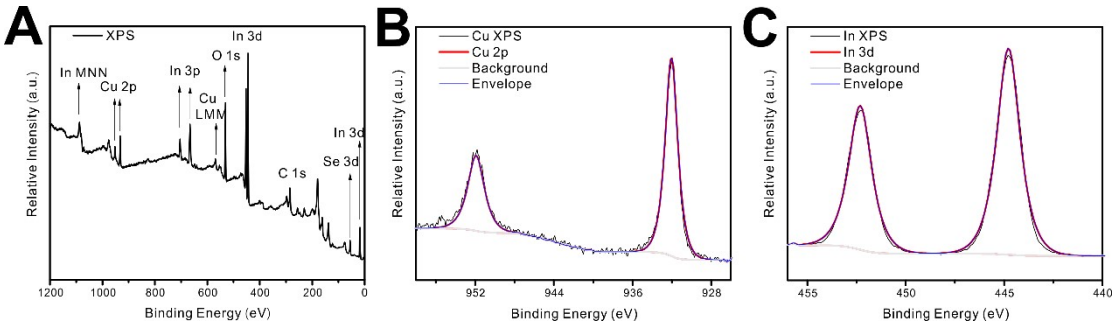

Figure S2 XPS results of CISe QDs. XPS (A), Cu 2p (B) and In 3d (C) of CISe QDs.

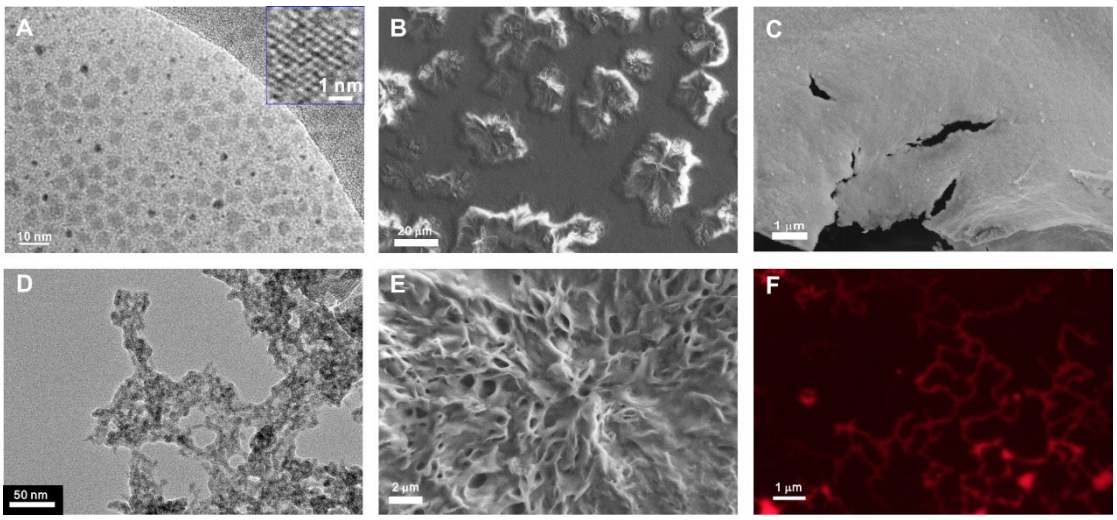

Figure S3 Characterization of CISe QDs and Zn-CISe aerogel. (A) TEM, and (B) SEM of CISe QDs (The droplets dry on the silicon wafer). (C) SEM of CISe QDs solid (freeze-dried). (D) TEM of Zn-CISe solid (After freeze-drying, Zn-CISe solid was dispersed in ethanol and dropped on the copper wire for testing). (E) SEM of Zn-CISe QDs gel (The droplet dries on the silicon wafer). (F) Fluorescent image of the fibers of Zn-CISe gel (The low concentration droplet dries on the slide).

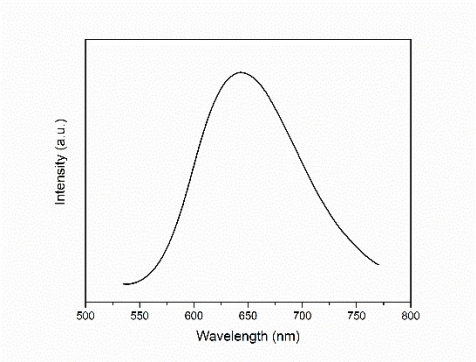

Figure S4 The PL of Zn-CISe gel stored at 4℃ for 1 year. (the concentrations of MPA, the ratio of Zn/In, and pH are 12 mM, 3, and 10.5, respectively.)

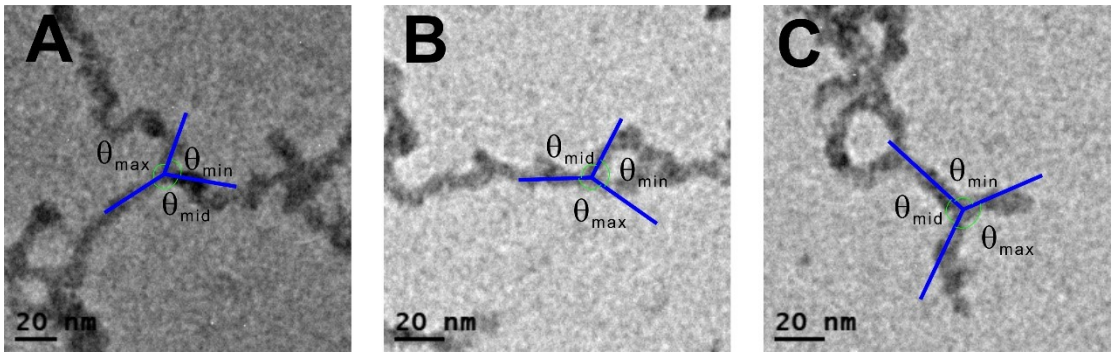

Figure S5 Degree of triangle branch angle of Figure 1D in (A) network inside, (B) cycle, and (C) rail end.

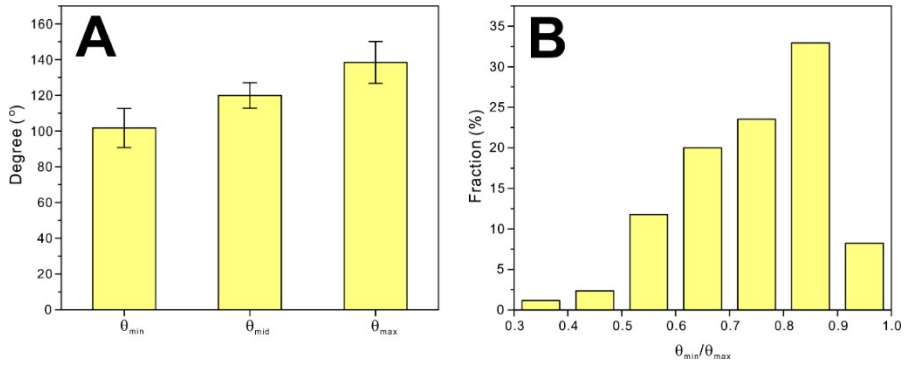

Figure S6 Statistics of degree of triangle branch angle (A) and $\theta_{min}/\theta_{max}$ (B) of Figure 1D.

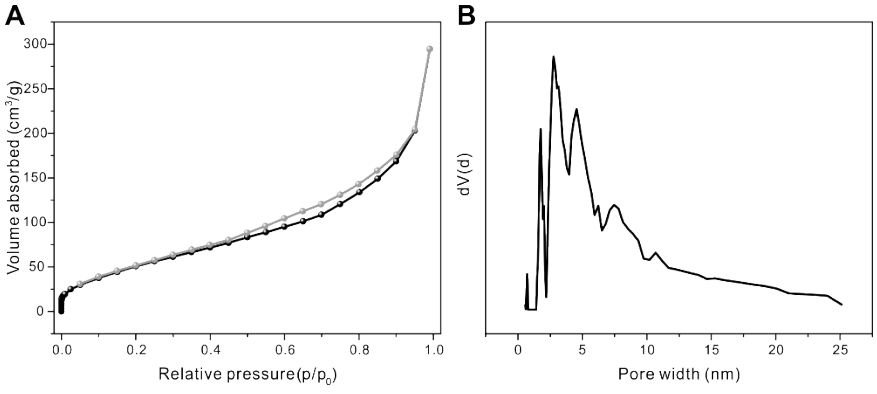

Figure S7 N_2 physisorption isotherm (A) and pore size distributions (B) of the Zn-CISe aerogel.

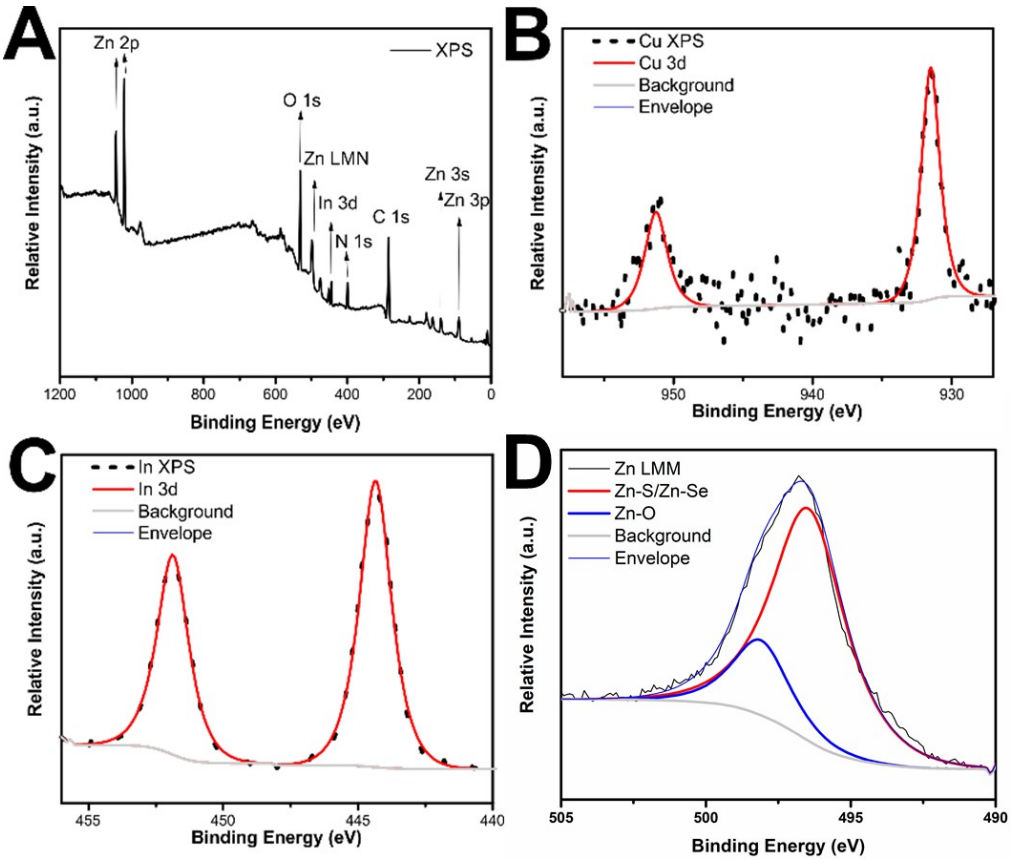

Figure S8 XPS results of Zn-CISe aerogel. (A) XPS, (B) Cu 2p, (C) In 3d and (D) Zn LMM of Zn-CISe aerogel.

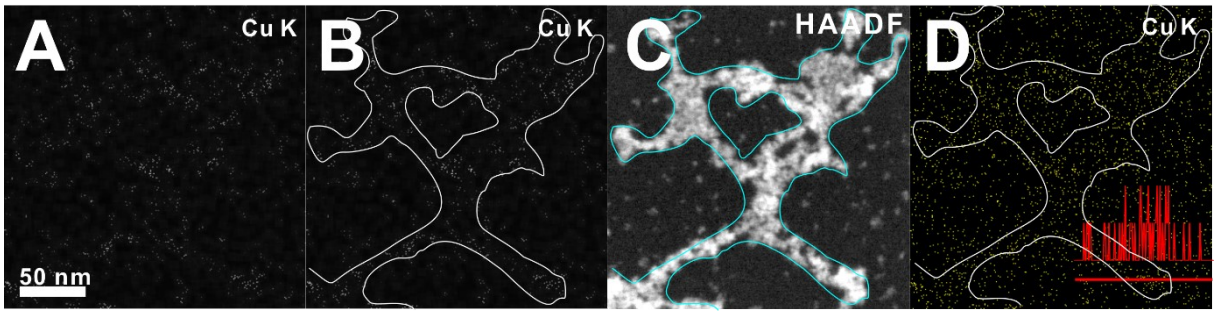

Figure S9 The images of distribution of Cu K. (A)and (B) The images of distribution of Cu K (processed by MATLAB). HAADF-STEM image (C) and Cu K mapping image (D) of Zn-CISe gel. (D) inset: The red polyline is the copper distribution on the red line.

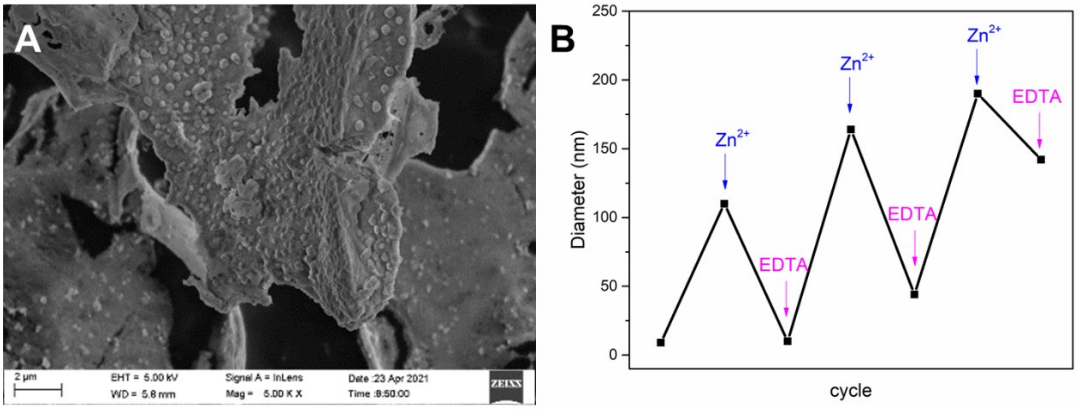

Figure S10 (A) SEM image of Zn-CISe gel with the addition of EDTA (freeze-drying). (B) The hydrated particle size of CISe QDs changes with the addition of Zn^{2+} or EDTA.

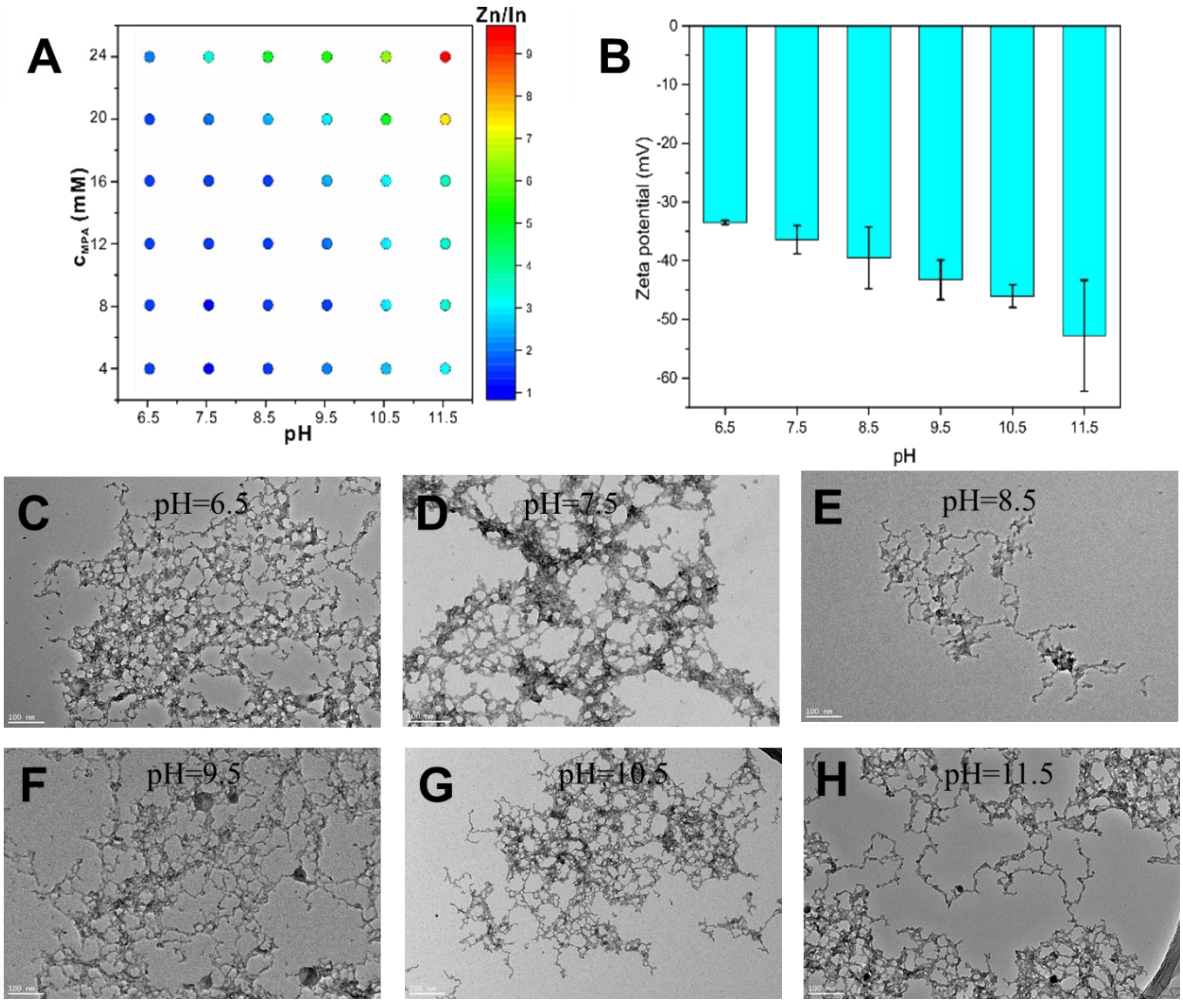

Figure S11 (A) The formation of Zn-CISe QDs gel under various concentrations of MPA, the ratio of Zn/In, and pH. (B) The zeta potential of CISe QDs (the concentrations of MPA is 12

mM). (C) TEM of Zn-CISe QDs gel (the concentrations of MPA, the ratio of Zn/In, and pH are 12 mM, 0.5, and 6.5, respectively). (D)TEM of Zn-CISe QDs gel (the concentrations of MPA, the ratio of Zn/In, and pH are 12 mM, 0.5, and 7.5, respectively). (E)TEM of Zn-CISe QDs gel (the concentrations of MPA, the ratio of Zn/In, and pH are 12 mM, 1, and 8.5, respectively). (F)TEM of Zn-CISe QDs gel (the concentrations of MPA, the ratio of Zn/In, and pH are 12 mM, 1.5, and 9.5, respectively). (G)TEM of Zn-CISe QDs gel (the concentrations of MPA, the ratio of Zn/In, and pH are 12 mM, 3, and 10.5, respectively). (H)TEM of Zn-CISe QDs gel (the concentrations of MPA, the ratio of Zn/In, and pH are 12 mM, 3, and 11.5, respectively).

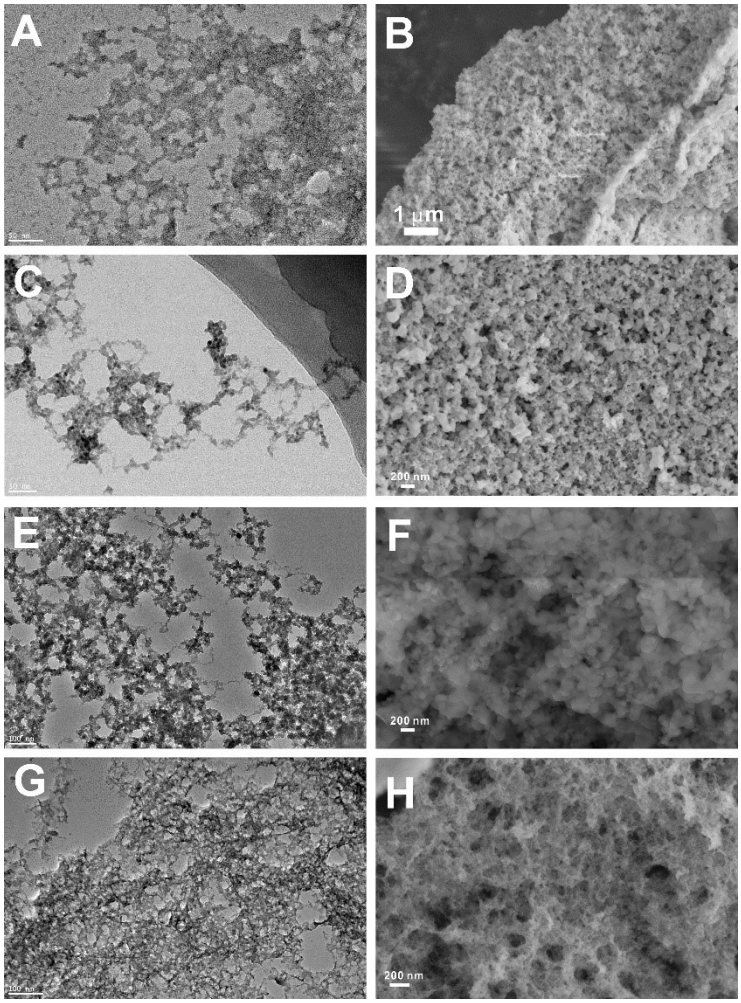

Figure S12 Metal ions induced CISe QDs self-assembly. TEM (A, C, E, and G) and SEM (B, D, F, and H) images of Ni-CISe aerogel, Pb-CISe aerogel, Fe-CISe aerogel, and Al-CISe aerogel,

respectively.

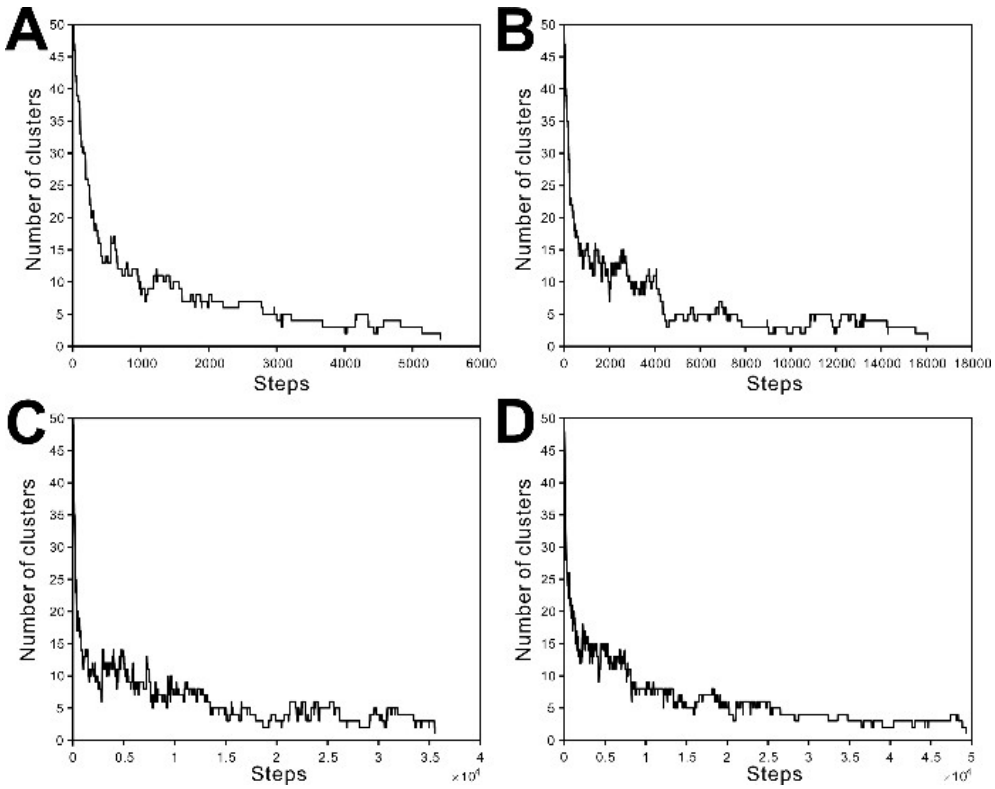

Figure S13 MC simulations for systems with various Zn^{2+} concentrations (f=100%). Typical MC simulations of the systems with Zn^{2+} concentrations: (A) $50c_0$, (B) $10c_0$, (C) $5c_0$, and (D) c_0.

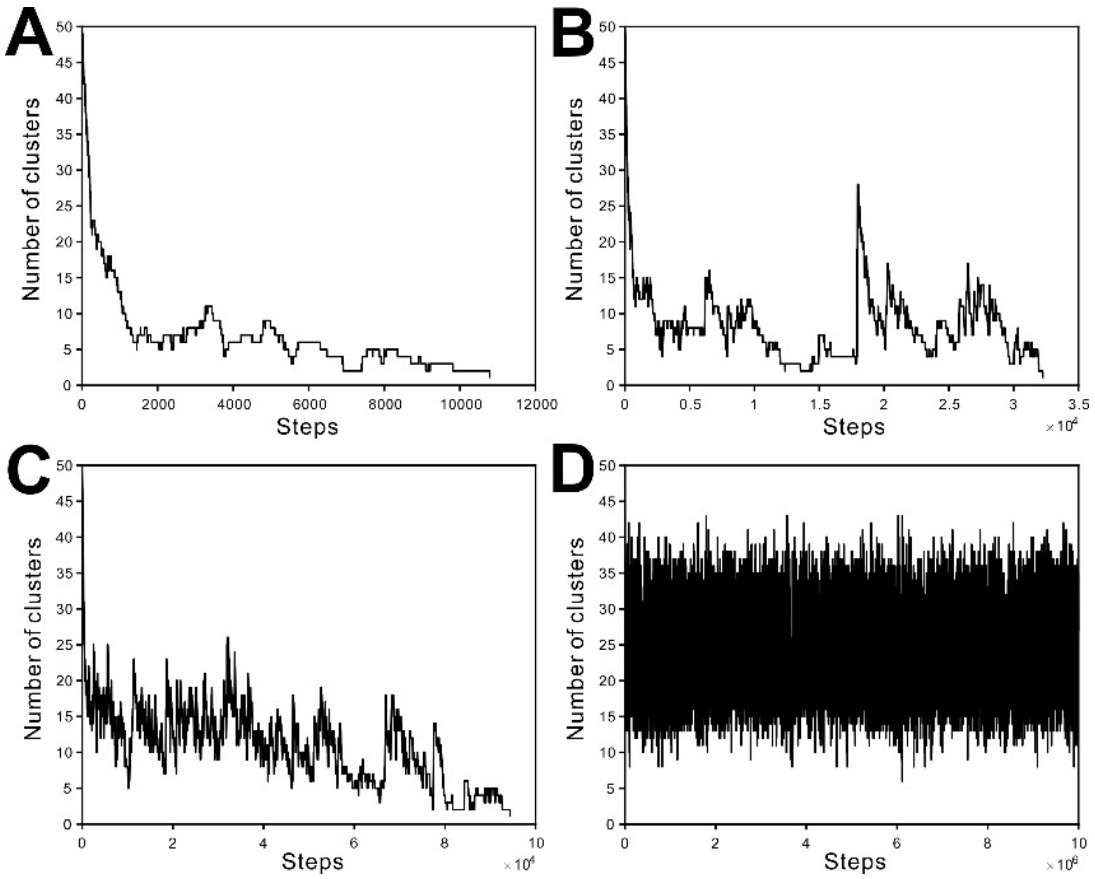

Figure S14 MC simulations for systems with various Zn^{2+} concentrations (f=99%). Typical MC simulations of the systems with Zn^{2+} concentrations: (A) $50c_0$, (B) $10c_0$, (C) $5c_0$, and (D) c_0.